

EXPERIMENTAL and modeling studies have accumulated strong evidence suggesting that A-currents control firing rates in invertebrate neurons. However, the direct demonstration of a similar role remains to be established in vertebrate neurons. We tested this possibility in a simulated neuron embedded with a generic model of vertebrate A-currents. Under simulated current-clamp protocols, the generic A-current produced a modest frequency reduction (15 Hz) that was constant within all firing frequencies. Modifications in steady-state properties of the A-current model within known physiological ranges annihilated or dramatically increased firing frequency reduction. These results suggest that the influence of A-currents on firing frequency should differ strongly among vertebrate neurons, and that modulations influencing A-currents provide a powerful control over the excitability of vertebrate neurons. *NeuroReport* 10:2773–2777 © 1999 Lippincott Williams & Wilkins.

Key words: A-current; Excitability types; Firing frequency; Modulatory influences; Vertebrate neurons

Diversity of firing frequency control by A-currents in vertebrate neurons: a modeling study

Bruno Delord

INSERM U483, Université Pierre et Marie Curie, Boite 23, 9 quai Saint-Bernard, 75005 Paris, France

Introduction

A wide variety of invertebrate and vertebrate cells are endowed with A-currents [1], a family of outward voltage-dependent potassium currents. A-conductances generally display very fast activation from subthreshold potentials, fast (but slower) inactivation with strong inactivation at action potential (AP) threshold, and large removal of inactivation with hyperpolarization from threshold. Functionally, A-currents have been attributed a role in AP repolarization [2], synaptic transmission efficacy [3] and control of transient excitability upon depolarization [4]. Moreover, A-currents are very often attributed a central role in regulating firing frequency [1,5,6].

Invertebrate somata and axons can fire at very low rates (typically < 10 Hz). This feature is accounted for by models incorporating A-currents [7,8] but not by the Hodgkin–Huxley model [9]. However, modified versions of the Hodgkin–Huxley model [10] are able to produce slow firing in the absence of A-current. Furthermore, some modeling evidence has shown that firing frequency reduction *per se* does not constitute an unconditional feature of all A-conductances. Rush and Rinzel [9] showed that the A-conductance described in Connor *et al.* [8] produced low rates only because of its atypical biophysical characteristics.

A-conductances have been observed in numerous vertebrate neurons [4], where they can dominate the overall potassium conductance [11]. Some experi-

mental data suggest that A-currents can reduce firing frequency [12,13]. However, a direct demonstration of this role remains to be established [6]. Moreover, conductance models for AP generation in vertebrate neurons display arbitrarily low frequency firing independent of the presence of A-conductances [14]. Thus, we aimed to determine the exact effect of A-currents on firing frequency of vertebrate neurons. We constructed a generic A-current model that captured the typical biophysical features of vertebrate A-currents and analyzed its effects on firing behavior in an isopotential neuron model endowed with AP conductances. As biophysical characteristics of A-conductances span large ranges and are subject to numerous modulatory influences [5] we performed a systematic parameter study in order to obtain a functional account of the biophysical variability found among vertebrate A-currents.

Materials and Methods

The role of A-currents in discharge behavior was evaluated in an isopotential neuron model that was designed to reproduce the basic electrophysiological behavior of vertebrate neurons. The membrane potential V obeyed

$$C \frac{dV}{dt} = -(I_{Na} + I_K + I_A + I_{leak}) + I_{app}$$

where the membrane capacitance was $1 \mu\text{F cm}^{-2}$. The leakage current was $I_{leak} = g_{leak}(V - E_{leak})$,

where $E_{leak} = -70$ mV and $g_{leak} = 0.05$ mS cm⁻² (passive time constant $\tau = 20$ ms). I_{app} represented an extrinsic current applied to the neuron model. The model of AP conductances was as in Lytton and Sejnowski [15] with $g_{Na} = 10$ mS cm⁻², $g_K = 2.5$ mS cm⁻², $E_{Na} = 45$ mV and $E_K = -85$ mV; AP threshold situated at ~ -50 mV.

A-currents have been characterized in a wide variety of vertebrate neurons, where they are usually distinguished from slowly-inactivating potassium currents by a lower affinity to 4-aminopyridine and much faster kinetics. In mammals, A-currents probably flow through K⁺ channels encoded by homologs of the *Drosophila* Shaker and Shal gene subfamilies (mShak and mShal), as the channels produced by these mammalian genes carry potassium currents sharing strong similarities with A-currents [16,17]. In order to determine the representative parameters used in the generic model presented below, we only considered reports that provided fully quantified descriptions of the A-conductances, in the cerebral cortex [18], thalamus [19], cerebellum [11], striatum [20], suprachiasmatic nucleus [21], laterodorsal tegmental nucleus [22] and nodose ganglia [23]. The generic A-current was modeled as $I_A = g_A a^3 b (V - E_A)$. Activation and inactivation variables followed first order kinetics: $dx/dt = (x_{\infty}(V) - x)/\tau_x$, $x = \{a, b\}$, where $x_{\infty}(V) = 1/(1 + \exp((V_x - V)/k_x))$. In vertebrate conductances, threshold for activation ($a_{\infty}(V) = 0.1$) ranges from -60 mV to -50 mV. Inactivation rolls off ($b_{\infty}(V) = 0.1$) in the range of -60 mV/ -40 mV. Compared with invertebrate A-conductances, vertebrate A-conductances activate at more hyperpolarized potentials but inactivate in a similar range of potentials [9]. As a result, vertebrate currents display a higher window component at subthreshold potentials. Generic parameters for activation and inactivation steady-state curves (see Fig. 1A) were taken (in mV): $V_a = -50$, $k_a = 10$, $V_b = -70$, $k_b = -7$. As voltage-independent time constants were used, we considered reported mean values at subthreshold potentials to characterize gating particle dynamics. Time constants were evaluated by fitting current-clamp data in Surmeier *et al.* [20]. Activation time constants generally approximate 1 ms, but values up to 10 ms can be found [21]. Inactivation time constants principally lay between 10 ms and 50 ms. We used $\tau = 1$ ms and $\tau_b = 25$ ms. Maximal A-conductances lie in the range 0.1 to 10 mS cm⁻², with most values > 1 mS cm⁻²; A-current reversal potentials span from -85 mV to -60 mV. We chose $g_A = 2.5$ mS cm⁻² and $E_A = -75$ mV as conservative estimations.

In the present model, firing emerged with zero steady-state firing frequency in response to I_{app} , and as full spikes situated around an unstable stationary

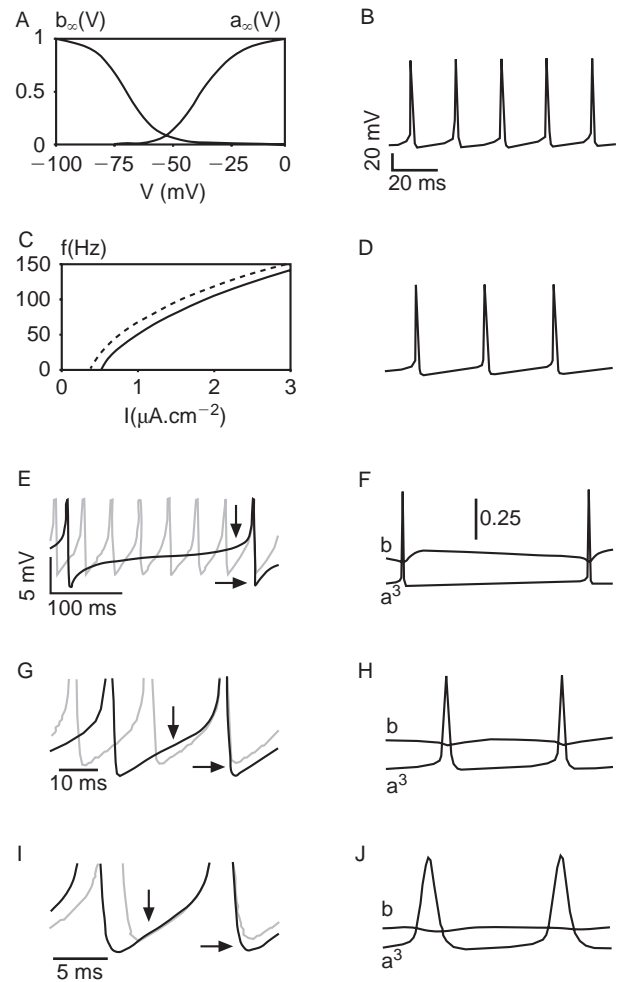


FIG. 1. Firing frequency control with the generic A-current model. **(A)** Activation ($a_{\infty}(V)$) and inactivation ($b_{\infty}(V)$) steady-state voltage dependencies. **(B)** Repetitive firing (50 Hz) with no A-current in response to $I_{app} = 0.75$ μ A cm⁻². **(C)** The steady-state frequency-current relationship of the model with $g_A = 2.5$ mS cm⁻² (solid curve) was shifted by ~ 15 –20 Hz compared to that obtained without A-current (dashed curve). **(D)** Repetitive firing (33 Hz) with $g_A = 2.5$ mS cm⁻² in response to an applied current identical to that in (B). **(E)** At low firing rate (4 Hz; $I_{app} = 0.5$ μ A cm⁻²), I_A decreased depolarization slope and enhanced action potential repolarization (black trace, arrows), compared to when I_A was absent (gray trace). **(F)** Activation and inactivation of the A-current corresponding to the voltage (black) trace with I_A in (E). Activation and inactivation are respectively computed as the quantities a^3 and b in the model described in the Materials and Methods section. Note the strong activation upon each action potential and the deinactivation after each spike. **(G)** At intermediate rates (33 Hz; $I_{app} = 0.75$ mS cm⁻²), I_A effect on repolarization was similar to that at low rates but the effect on depolarization slope was attenuated. Results are presented as in (E). **(H)** Note that inactivation varied less than at low frequency. Results are presented as in (F). **(I)** At high firing rates (82 Hz; $I_{app} = 1.5$ μ A cm⁻²), I_A was too weak during inter-spike intervals to reduce depolarization slope, but it still enhanced action potential repolarization (compare with E and G). **(J)** Note that inactivation was almost constant in this case. Results are presented as in (F). Spikes truncated in (E), (G) and (I). Potential calibration bar in (E) applies to (G) and (I). Dimensionless calibration bar for activation and inactivation in (F) applies to (H) and (J). Time calibration bar in (E), (G) and (I) applies respectively to (F), (H) and (J).

solution, indicating a homoclinic bifurcation at saddle-node [24]. This was true both in the absence and in the presence of the A-current, and with all biophysical parameter sets used in the study (see below).

Results

With no A-conductance ($g_A = 0$), the neuron model fired repetitively when depolarized by a constantly applied current of sufficient amplitude (Fig. 1B). The steady-state frequency–current relationship (f/I_{app}) displayed a classical increasing curve with firing emerging from zero frequency (Fig. 1C; dashed line). With $g_A = 2.5 \text{ mS cm}^{-2}$ firing frequency was reduced by $\sim 15\text{--}20 \text{ Hz}$ at all applied currents so that the f/I_{app} curve was shifted rightward (Fig. 1C; solid line). An example of discharge with $g_A = 2.5 \text{ mS cm}^{-2}$ is presented in Fig. 1D in response to a current similar to that applied in Fig. 1B. We studied the way repetitive discharge was slowed by the A-conductance in a wide range of firing rates. Activation dynamics were similar at all firing frequencies (see Fig. 1F,H and J for examples at low, intermediate, and high firing rates). During inter-spike intervals (ISIs), activation remained small but increased as membrane potential depolarized to the next AP. Because of its fast activation kinetics, the A-conductance strongly activated and then quickly deactivated throughout the action potentials. Thus, I_A peaked during APs, which amplified repolarization after each spike (Fig. 1E,G,I) and lengthened the time needed to reach threshold for the next AP. Contrary to activation, inactivation dynamics depended on firing frequency. At low rates, deinactivation due to action potential repolarization was followed by slow inactivation during depolarization (Fig. 1F). However, at higher frequencies, inactivation was almost constant during the entire firing cycle (Fig. 1H,J). In all cases, inactivation remained significant and allowed steady A-currents during ISIs. At frequencies $< 50 \text{ Hz}$, I_A decreased the depolarization slope, which contributed to lengthened ISIs (Fig. 1E,G). At high firing rates, however, I_A was not strong enough to counteract the applied current during ISIs and the depolarization slope was similar with or without A-current (Fig. 1I). In this case, firing frequency reduction was exclusively produced by enhanced repolarization due to the strong activation upon action potentials.

A systematic parameter study revealed that firing frequency control by the generic A-current was sensitive to variations of parameter values within physiological ranges. We first tested the influence of g_A on frequency reduction. When g_A was set to 0.5 mS cm^{-2} I_A produced almost no effect on firing frequency ($< 5 \text{ Hz}$; Fig. 2A). However, with $g_A = 10 \text{ mS cm}^{-2}$ it produced a frequency reduction of $\sim 50 \text{ Hz}$ through a large shift of the f/I_{app} curve (Fig. 2A). The model revealed that the effect of I_A was very sensitive to voltage dependencies of the A-conductance. Shifting the $a_\infty(V)$ curve rightward

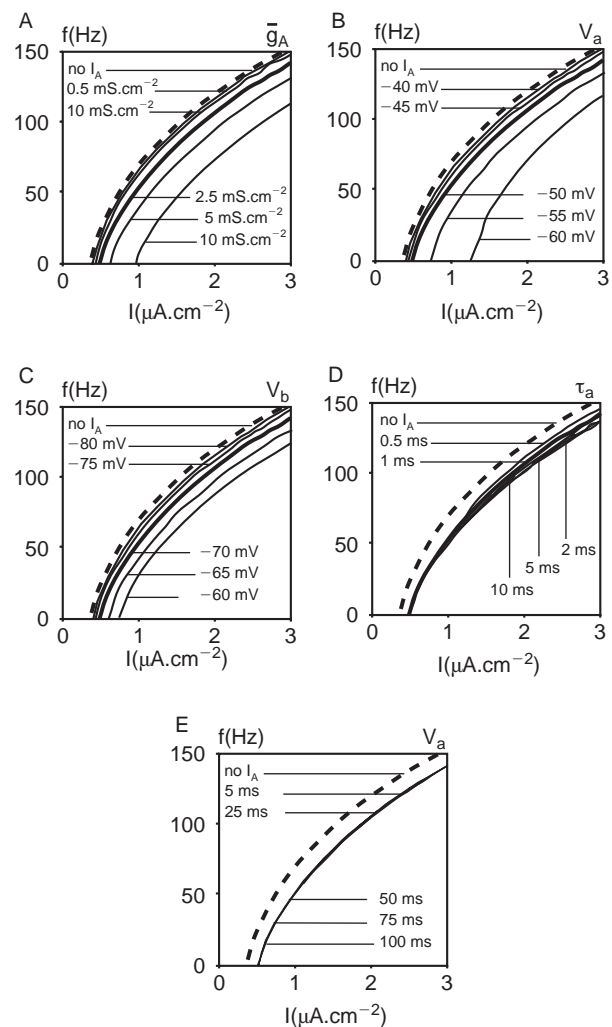


FIG. 2. Diversity of firing frequency control by A-current models with biophysical parameters varying within physiological ranges (see Materials and Methods). Each graph represents the steady-state frequency–current relationships of the neuron model without I_A (dashed curve), with the generic I_A model (heavy black curve) and with I_A models with modified biophysical parameters (thin black curves). (A–C) Modifications of steady-state properties of I_A strongly altered firing frequency control. (A) Changes in maximal A-conductance. (B) Shifts of the voltage-dependency for activation. (C) Shifts of the voltage-dependency for inactivation. (D,E) Modifications of A-conductance dynamics had restricted effects on steady-state frequency–current relationship. (D) Changes in activation time constant. (E) Changes in inactivation time constant.

(i.e. activation started at more depolarized potentials; Fig. 2B) or the $b_\infty(V)$ curve leftward (i.e. inactivation completed at more hyperpolarized potentials; Fig. 2C) by 10 mV almost annihilated the effects of I_A on firing frequency. Opposite shifts of the same amplitudes led to displacements of the f/I_A curve to strong frequency reductions (respectively $\sim 50 \text{ Hz}$ and $\sim 30 \text{ Hz}$; Fig. 2B,C). Contrary to steady-state properties, changes in A-current dynamics did not affect frequency. The activation time constant had a very limited influence on frequency reduction and this effect was restricted to high frequencies ($> 50 \text{ Hz}$; Fig. 2D). Furthermore, the

inactivation time constant had no effect on frequency reduction (Fig. 2E).

Discussion

The present results, obtained in a vertebrate neuron model, support previous experimental and modeling studies demonstrating the central influence of invertebrate A-currents on firing frequency [7–9]. In invertebrates, A-currents have been demonstrated to support class I excitability, where firing emerges from zero frequency [7,8,25]. In these cells, A-currents modify encoding capabilities by extending frequency transduction to arbitrarily low firing rates. In vertebrate neurons, models for AP generation predict firing from zero frequency, even in the absence of A-currents [14]. Nevertheless, our study suggests that vertebrate A-currents are capable to controlling firing behavior. This control is expressed as shifts in the stimulus range for frequency encoding and therefore strongly differs from that shown in invertebrates.

In the present model of vertebrate A-currents, mechanisms responsible for firing frequency control departed from descriptions in invertebrate membranes [7–9]. In invertebrate cells, inactivation slowly decreases after partial recovery upon AP undershoot and temporally overlaps with activation during subsequent depolarization. This results in a transient conductance delay occurrence of the next AP. This dynamic interaction was shown to depend notably upon the inactivation time constant [8,9]. In the generic vertebrate A-current model, a similar sequence of events was observed only at very low firing rates. However, at most firing frequencies, inactivation approximated a constant value and the activation mostly determined the influence of I_A on firing frequency through its effects on action potential repolarization and inter-spike interval depolarization slope (see Results). As a general property, the present mechanisms differed from descriptions in invertebrates in that they almost exclusively depended on steady-state characteristics of the A-conductance, consistent with experimental observations made in vertebrate neurons [11,22]. Nevertheless, the results presented here support the observation of Connor and Stevens [7] that slow dynamics can be achieved in systems endowed with fast time constants.

Modifications of A-current steady-state properties within known physiological ranges produced strong variations in the control of firing frequency (5–50 Hz). These results suggest that firing frequency control does not represent an unconditional function of A-currents in vertebrate neurons. Rather, A-currents should display very different degrees of

influence on firing frequency among vertebrate neurons, given their biophysical diversity *in vitro*. For example, Banks *et al.* [26] have shown *in vitro* that A-currents display layer-specific biophysical properties in the piriform cortex. Using their parameters in our model, we found that the A-current of layer II pyramidal neurons induced a frequency reduction (~ 40 Hz) 3-fold to that found with the A-current of endopiriform nucleus neurons (10–15 Hz). This difference in firing frequency control, together with other effects [26], could contribute to the susceptibility of the endopiriform nucleus to induce epileptiform activity. Finally, evidence has been provided that steady-state properties of vertebrate A-currents can be modulated by Zn^{2+} ions [27], GABA_B agonists [28], acetylcholine [29] and noradrenaline [30]. In this perspective, the present results suggest that A-currents constitute efficient targets for regulating vertebrate neuronal excitability through molecular and electrical modulatory influences tuning their biophysical properties.

Conclusion

We investigated the role of vertebrate A-currents on firing frequency in a neuron model embedded with a generic potassium current that reproduced typical biophysical characteristics of vertebrate A-currents. In response to constant depolarizing inputs, the generic A-current reduced firing frequency through enhanced action potential repolarization and slowed depolarization between spikes. The underlying mechanisms differed from those shown in invertebrate neurons, as they relied on steady-state rather than on dynamic properties of the A-conductance. A parameter study showed that biophysical characteristics of vertebrate A-conductances lie in a parameter region most favorable to large changes in firing frequency control. Together, these results suggest that the influence of A-currents on firing frequency in vertebrate neurons is a conditional property that depends on their biophysical properties. As a consequence, the precise tuning of the biophysical characteristics of A-currents by modulatory influences may represent a powerful means for regulating overall excitability of vertebrate neurons.

References

1. Rogawski M. *Trends Neurosci* **8**, 214–219 (1985).
2. Belluzzi O, Sacchi O and Wanke E. *J Physiol (Lond)* **358**, 91–108 (1985).
3. Ducreux C and Puizillout JJ. *J Physiol (Lond)* **486**, 439–451 (1995).
4. Golowasch J, Buchholtz F, Epstein IR *et al.* *J Neurophysiol* **67**, 341–349 (1992).
5. Rudy B. *Neuroscience* **25**, 729–749 (1988).
6. Storm JF. *Prog Brain Res* **83**, 161–187 (1990).
7. Connor JA and Stevens CF. *J Physiol* **213**, 31–53 (1971).
8. Connor JA, Walter D and McKnown R. *Biophys J* **18**, 81–102 (1977).
9. Rush ME and Rinzel J. *Bull Math Biol* **57**:6, 899–929 (1995).
10. Shapiro BI and Lenherr FK. *Biophys J* **12**, 1145–1158 (1972).
11. Bardoni R and Belluzzi O. *J Neurophysiol* **69**, 2222–2231 (1993).

12. Locke RE and Nerbonne JM. *J Neurophysiol* **78**, 2321–35 (1997).
13. Rathouz M and Trussell L. *J Neurophysiol* **80**, 2824–35 (1998).
14. Ermentrout GB. *Rep Prog Phys* **61**, 353–430 (1998).
15. Lytton WW and Sejnowski TJ. *J Neurophysiol* **66**, 1059–1079 (1991).
16. Stühmer W, Ruppersberg JP, Schröter KH, et al. *EMBO J* **8**:11, 3235–3244 (1989).
17. Pak MD, Baker K, Covarrubias M et al. *Proc Natl Acad Sci* **88**, 4386–4390 (1991).
18. Spain WJ, Schwandt PC and Crill WE. *J Physiol* **434**, 591–607 (1991).
19. Huguenard JR and McCormick DA. *J Neurophysiol* **68**, 1373–1383 (1992).
20. Surmeier DJ, Bargas J and Kitai ST. *Neurosci Lett* **103**, 331–337 (1989).
21. Bouskila Y and Dudek E. *J Physiol* **488**, 339–350 (1995).
22. Sanchez RM, Surkis A and Leonard C. *J Neurophysiol* **79**, 3111–3126 (1998).
23. McFarlane S and Cooper E. *J Neurophysiol* **66**, 1380–1391 (1991).
24. Kuznetsov Y. *Elements of Applied Bifurcation Theory*. Applied Mathematical Sciences, New York: Springer-Verlag, 1995: 112.
25. Connor JA. *J Neurophysiol* **38**, 922–932 (1975).
26. Banks MI, Haberly LB and Jackson MB. *J Neurosci* **16**, 3862–3876 (1996).
27. Song WJ, Tkatch T, Baranauskas G et al. *J Neurosci* **18**, 3124–3137 (1998).
28. Saint DA, Thomas T and Gage PW. *Neurosci Lett* **118**, 9–13 (1990).
29. Nakajima Y, Nakajima S, Leonard RJ et al. *Proc Natl Acad Sci USA* **83**, 3022–3026 (1986).
30. Aghanajian GK. *Nature* **315**, 501–504 (1985).

ACKNOWLEDGEMENTS: I thank E. Guigon for helpful comments and Cecilia Langram for correcting the English.

**Received 2 June 1999;
accepted 7 July 1999**